DMD Fast Forward. Published on January 6, 2010 as doi:10.1124/dmd.109.031179

DMD #31179

METABOLISM OF INTRAVENOUS METHYLNALTREXONE IN MICE, RATS, DOGS AND HUMANS

Appavu Chandrasekaran, Zeen Tong, Hongshan Li, John C. L. Erve, William DeMaio, Igor Goljer, Oliver McConnell, Yakov Rotshteyn, Theresa Hultin, Rasmy Talaat and JoAnn Scatina

Pharmacokinetics, Dynamics and Metabolism (A.C., Z.T., H.L., J.E., W.D., T.H., R.T., J.S.) and Discovery Analytical Chemistry (I.G., O.M.), Pfizer, 500 Arcola Road, Collegeville, PA 19426 and Progenics Pharmaceuticals, Inc. (Y.R.), 777 Old Saw Mill River Road, Tarrytown, NY 10591

Copyright 2010 by the American Society for Pharmacology and Experimental Therapeutics.

Running title: In vivo metabolism of methylnaltrexone

Corresponding author:

Appavu Chandrasekaran, PhD
Pharmacokinetics, Dynamics and Metabolism
Pfizer, Inc
500 Arcola Road
Collegeville, PA 19426
Phone: (484) 865-5333
Fax: (484)865-9403
E-mail: Chandra@wyeth.com

Numbers of pages: 28
Number of tables: 2
Number of Figures: 9
Number of references: 31
Number of words: Abstract: 201; Introduction: 235; Discussion: 1027.

Non-standard Abbreviations:

AAALAC, Association for Assessment and Accreditation of Laboratory Animal Care; AUC, Area Under Curve; CD-1, Cluster of Differentiation 1 A Small Gene Family; CD_3OD, d_4-methanol; D_2O, deuterium oxide; EDTA, Ethylenediamine tetraacetic acid; HPLC, High Performance Liquid Chromatography; ICFs, Informed Consent Forms; IRB, Institutional Review Board; LC/MS, Liquid Chromatography/Mass Spectrometry; LC/MS/MS, Liquid Chromatography/Mass Spectrometry/Mass Spectrometry; LSC, Liquid Scintillation Counter; MNTX, methylnaltrexone; $[M+H]^+$, Protonated molecule; *m/z,* mass-to-charge ratio; $NADP^+$, Nicotinamide Adenine Dinucleotide Phosphate; NADPH, Nicotinamide Adenine Dinucleotide Phosphate, reduced form; TFA, trifluoroacetic acid; UV, Ultraviolet.

ABSTRACT:

Methylnaltrexone (MNTX), a selective mu-opioid receptor antagonist, functions as a peripherally acting receptor antagonist in tissues of the gastrointestinal tract. This report describes the metabolic fate of [^{3}H]MNTX or [^{14}C]MNTX bromide in mice, rats, dogs and humans following intravenous administration. Separation and identification of plasma and urinary MNTX metabolites was achieved by HPLC-radioactivity detection and LC/MS. The structures of the most abundant human metabolites were confirmed by chemical synthesis and NMR spectroscopic analysis. Analysis of radioactivity in plasma and urine showed that MNTX underwent two major pathways of metabolism in humans: sulfation of the phenolic group to MNTX-3-sulfate (M2) and reduction of the carbonyl group to two epimeric alcohols, methyl-6α-naltrexol (M4) and methyl-6β-naltrexol (M5). Neither naltrexone nor its metabolite 6β-naltrexol were detected in human plasma following administration of MNTX, confirming an earlier observation that *N*-demethylation was not a metabolic pathway of MNTX in humans. The urinary metabolite profiles in humans were consistent with plasma profiles. In mice, the circulating and urinary metabolites included methyl-6β-naltrexol (M5), MNTX-3-glucuronide (M9), 2-hydroxy-3-*O*-methyl MNTX (M6) and its glucuronide (M10). MNTX-3-sulfate (M2), methyl-6β-naltrexol (M5), 2-hydroxy-3-*O*-methyl MNTX (M6) and MNTX-3-glucuronide (M9) were observed in rats. Dogs produced only one metabolite, MNTX-3-glucuronide (M9). In conclusion, MNTX was not extensively metabolized in humans. Conversion to methyl-6-naltrexol isomers (M4 and M5) and MNTX-3-sulfate (M2) were the primary pathways of metabolism in humans. MNTX was metabolized to a higher extent in mice than in rats, dogs, and humans. Glucuronidation was a major metabolic pathway in mice, rats and dogs, but not in humans. Overall, the data suggested species differences in the metabolism of MNTX.

Introduction

Methylnaltrexone bromide (MNTX, (5α)-17-(cyclopropylmethyl)-3,14-dihydroxy-17-methyl-4,5-epoxymorphinanium-17-ium-6-one) is a selective peripherally acting mu-opioid receptor antagonist. *In vitro* testing shows that MNTX binds to *mu* receptors at 8-fold higher potency than to kappa receptors and it does not interact with delta receptors. MNTX is a quaternary derivative of the opioid antagonist naltrexone (Brown and Goldberg, 1985). The addition of the methyl group to naltrexone at the nitrogen atom forms MNTX, an inherently positively charged compound with greater polarity and lower lipid solubility than naltrexone. MNTX is restricted from crossing the blood-brain-barrier in animals at pharmacologically relevant doses (Brown and Goldberg, 1985; Yuan et al., 1996; Yuan et al., 1998). MNTX prevents the inhibition of opioid-induced gut contractions in guinea pig ileum (Chen and Rosow, 2007). Studies in a variety of animal species have shown that peripherally or systemically administered MNTX blocks the peripherally mediated side effects of opioids, particularly their inhibition of gastrointestinal motility, with no effect on centrally mediated analgesia or opioid tolerance.

MNTX reverses the opioid-induced delay in both gastric emptying and transit time without affecting analgesia in human volunteers (Yuan et al., 1996; Yuan et al., 2002). In a randomized placebo-controlled study in long-term methadone users, MNTX was shown to induce laxation (Yuan et al., 2000). In a phase 3 clinical trial, subcutaneous injection of MNTX rapidly induced laxation in patients with advanced illness who were receiving opioid therapy for pain. In addition, MNTX treatment did not affect central analgesia or lead to opioid withdrawal (Thomas et al., 2008). RELISTOR® (methylnaltrexone bromide) is currently approved in the US as an

injectable medication for the treatment of opioid-induced constipation in patients with advanced illness who are receiving palliative care, when response to laxative therapy has not been sufficient, and is approved elsewhere around the world for similar indications.

A limited number of studies have been reported in the literature on the metabolism of MNTX in animals and humans (Kotake et al., 1989; Misra et al., 1987; Murphy et al., 2001; Kim et al., 1989). The focus of those studies was to evaluate the potential uptake into the brain in rats and the extent of demethylation in laboratory animals and humans. The data showed that the penetration of MNTX into the rat brain was restricted. MNTX was not demethylated to any significant extent in humans. Mice and rats had a slightly higher capability to *N*-demethylate MNTX than dogs or humans. The present studies were performed to determine the metabolism of radiolabeled MNTX in mice, rats, dogs and humans following intravenous administration.

Materials and Methods

Materials. [^{3}H]MNTX bromide salt (Lot SEL/1674) and [^{14}C]MNTX bromide salt (Lot 2108DCR005-1) were synthesized by Selcia Limited (Essex, UK). The radiochemical purity and the chemical purity (by UV detection) of the radiolabeled MNTX bromide were greater than 97%. The specific activity was 129.4 μCi/mg (158.4 μCi/mg as the free base) for [^{3}H]MNTX bromide and 125.1 μCi/mg (153.0 μCi/mg as the free base) for [^{14}C]MNTX bromide. Non-radiolabeled MNTX bromide salt (Lot H10207) was synthesized by Mallinckrodt, Inc. (Phillipsburg, NJ) and had a chemical purity of 100%. The structure of MNTX including the sites of ^{3}H and ^{14}C labels is shown in Figure 1. Unless indicated otherwise, when referring to [^{14}C]MNTX or MNTX, the free-base form is assumed. Sulfur trioxide-*N*-triethylamine complex, sodium borohydride, naltrexone, 6β-naltrexol hydrate, glucose-6-phosphate, β-nicotinamide adenine dinucleotide phosphate ($NADP^{+}$), glucose-6-phosphate dehydrogenase and β-glucuronidase (10,100 units/mg, type B-10 from bovine liver) were obtained from Sigma-Aldrich (Milwaukee, WI). Ultima Gold and Ultima Flo M scintillation cocktails were purchased from PerkinElmer Life and Analytical Sciences (Boston, MA). Solvents used for extraction and for chromatographic analysis were HPLC or ACS reagent grade and were purchased from EMD Chemicals (Gibbstown, NJ). Deuterium oxide (D_2O) and d_4-methanol (CD_3OD) were obtained from Cambridge Isotope Laboratories (Andover, MA).

Synthesis of MNTX Metabolites. MNTX-3-sulfate, the reference standard for MNTX metabolite M2, was synthesized by method of Jones et al. (Jones et al., 2005). Briefly, MNTX bromide (74 mg) was dissolved in dioxane (20 mL) in a water bath (50^{o}C). Sulfur trioxide-*N*-triethylamine complex (310 mg) was added to the solution and the mixture was maintained at 50^{o}C for 2 h. The dioxane was decanted and the precipitate on the glass was dissolved in 1 mL

of a mixture of water and methanol (1:1, v/v). Purification was accomplished by UV detection using a HPLC method described later. The purified fraction was analyzed by LC/MS, dried under a nitrogen stream in a TurboVap LV evaporator (Caliper Life Sciences, Hopkinton, MA) and reconstituted in CD_3OD for NMR spectroscopic analysis.

Methyl-6α-naltrexol and methyl-6β-naltrexol, the reference standards for MNTX metabolites M4 and M5, respectively, were synthesized by the method of Malspeis for naltrexone (Malspeis et al., 1975). Briefly, MNTX (100 mg) was dissolved in 95% ethanol (5 mL), and the alcoholic solution was cooled in an ice bath. Sodium borohydride (25 mg) was slowly added with stirring, and the mixture was brought to room temperature and stirred for an additional 2 h. The solvent was evaporated under a nitrogen stream in a TurboVap LV evaporator (Caliper Life Sciences) and the residue was dissolved in water (2 mL). After acidification with 1N HCl, aliquots of the solution were injected onto an HPLC column and the products were isolated after UV detection using the HPLC method described later. The purified fraction was analyzed by LC/MS, dried under a nitrogen stream in a TurboVap LV evaporator (Caliper Life Sciences), and reconstituted in CD_3OD for NMR spectroscopic analysis.

Animal Studies. Male CD-1 mice and Sprague-Dawley rats were purchased from Charles River Laboratories (Wilmington, MA). The dogs were from Wyeth in-house colony. The dose was prepared in 0.9% saline for all non-clinical species. Twenty-four non-fasted male mice, weighing from 26.5 to 34.8 g at the time of dosing, were given a single 5 mg/kg (400 μCi/kg) dose of [^{14}C]MNTX in a volume of 5.0 mL/kg via the tail vein. Sixteen non-fasted male rats, weighing 294 to 336 g at the time of dosing, were given a single 5 mg/kg (300 μCi/kg) dose of [^{3}H]MNTX in a volume of 1.0 mL/kg via the tail vein. Four non-fasted male beagle dogs,

weighing 8.7 to 12.2 kg at the time of dosing, were given a single 5 mg/kg (50 μCi/kg) dose of [^{3}H]MNTX at a volume of 1.0 mL/kg via the saphenous vein. Mice were kept as a group for each time point, and rats and dogs were kept individually in metabolic cages. All animal housing and care was conducted in Association for Assessment and Accreditation of Laboratory Animal Care (AAALAC) accredited facilities. Animal care and use for this investigation was approved by the Wyeth Institutional Animal Care and Use Committee. Animal rooms were maintained on a 12-hour light and dark cycle. Animals were provided food and water *ad libitum*.

Blood samples were collected at 0.25, 1, 4 and 24 h after dose administration from mice (6/time point) and rats (4/time point) by cardiac puncture and from the jugular vein of dogs. Potassium EDTA was used as the anticoagulant and plasma was immediately harvested from the blood by centrifugation at 4°C. Urine samples were collected from animals on dry ice at 0-24 h post-dose. All biological specimens were stored at approximately -70°C until analysis.

Human Study. This study was an open-label, phase I, single dose study of the pharmacokinetics, mass balance and disposition of intravenously administered ^{14}C-methyltrexone in normal, healthy volunteers. Six healthy male human subjects were administered a single 0.3 mg/kg (100 μCi/subject) intravenous dose of [^{14}C]MNTX. Samples of expired CO_2 for the determination of radioactivity were collected every 15 minutes between 0 and 4 h post-dosing, and every 30 minutes between 4 and 8 h post-dosing. Plasma samples were collected pre-dose and at 2, 5, 15, 30, and 45 min, and 1, 1.5, 2, 3, 4, 5, 6, 8, 10, 12, 16, 24, 36, 48, 72, 96, and 120 h post-dose. Urine samples were collected at 0-24, 24-48, 48-72, 72-96, 96-120 and 120-144 h intervals post-dose. Fecal samples were collected at 24 hr intervals through 168 h post-dose. The plasma and urine samples were stored at –70°C until analysis for

metabolite profiles. The protocol, the investigator's brochure, and the informed consent forms (ICFs) were submitted to the study site institutional review board (IRB) for review and written approval. Subsequent amendments to the protocols and/or any revisions to the ICFs were submitted for IRB review and written approval. This study was conducted in accordance with ethical principles that have origins in the Declaration of Helsinki and in any amendments that were in place when the study was conducted. This study were also designed and performed in compliance with Good Clinical Practice (GCP). Written informed consent was obtained from all subjects before their enrollment. WinNonlin Enterprise (version 4.1, Pharsight Corp, Mountain View, CA) was used to calculate the area under the curve (AUC) values.

Determination of Radioactivity. Aliquots of plasma (50 μL) and urine (200 μL) samples were analyzed for radioactivity with a Tri-Carb Model 3100 TR/LL liquid scintillation counter (PerkinElmer) using 10 mL of Ultima Gold as the scintillation fluid. Radioactivity detection for HPLC was accomplished with a TopCount microplate reader or an in-line Flo-One radioactivity flow detector (PerkinElmer). For plasma samples, the eluent was collected at 10 second intervals into 96-well LumaPlates (PerkinElmer). The plates were dried overnight in an oven at 40°C and analyzed by the TopCount NXT radiometric microplate reader. For urine samples, a Flo-One β Model A525 radioactivity flow detector (PerkinElmer) with a 250 μL LQTR flow cell and a Waters model 996 photodiode array UV detector (Waters Corp., Milford, MA) set to monitor 280 nm were used for data acquisition. The flow rate of Ultima Flo M scintillation fluid was 3.0 mL/min, providing a mixing ratio of scintillation cocktail to mobile phase of about 5:1.

Sample Preparation. Animal plasma samples collected at 0.25, 1 and 4 h and human plasma samples collected at 2, 5, 15, 30, and 45 min, and 1, 1.5, 2 and 4 h post-dose were pooled across

individuals by combining an equal volume for each time point. Aliquots (3.0 mL) of the pooled plasma were mixed with 3.0 mL of methanol, placed on ice for about 10 min, and then centrifuged at 4°C. The supernatant was transferred to a clean tube. The protein pellets were extracted twice with 3.0 mL of methanol. The supernatants from precipitation and extraction were pooled, mixed, and evaporated at 22°C under nitrogen in a TurboVap LV evaporator (Caliper Life Sciences) to about 0.8 mL. The concentrated extract was centrifuged, the supernatant volume measured and the extraction efficiency was determined by analyzing duplicate 10 µL aliquots for radioactivity concentrations. The extraction method recovered greater than 80% of plasma radioactivity. An aliquot (200 µL) of the supernatant was injected onto the HPLC column and fractions were collected for determination of radioactivity as described above. The 24 h plasma samples collected from animals and the human plasma samples collected after 4 h post-dose were not analyzed for metabolite profiles due to low radioactivity concentrations. Urine samples were analyzed by direct injection into the HPLC system.

High Performance Liquid Chromatography (HPLC). A Waters model 2695 HPLC system (Waters Corp.) with a built-in autosampler was used for analysis. Separations were accomplished on a Luna C18(2) column (250 x 4.6 mm, 5 µm) (Phenomenex, Torrance, CA). The sample chamber in the autosampler was maintained at 4°C, while the column was at 40°C. The mobile phase consisted of 0.05% trifluoroacetic acid (TFA) in water (A, v/v) and 0.05% TFA in methanol (B, v/v) and was delivered at 0.6 mL/min. The linear HPLC gradient started at 10% B and increased to 20% over 25 minutes and then increased to 30% over 5 minutes. Flo-One analytical software (version 3.65, PerkinElmer) was utilized to integrate the radioactive peaks. DataFlo software utility (beta version 0.55, PerkinElmer) was used to convert ASCII files

from the TopCount NXT microplate counter into CR format for processing in Flo-One analysis software.

Mass Spectrometry. Plasma extracts and urine samples were analyzed by LC/MS for metabolite characterization. Potential *N*-demethylation of MNTX in humans was investigated by analyzing plasma samples for naltrexone and 6β-naltrexol. The limit of detection was 6 ng/mL for naltrexone and 3 ng/mL for 6β-naltrexol. An Agilent Model 1100 HPLC system including a binary pump and diode array UV detector (Agilent Technologies, Palo Alto, CA) was used with the mass spectrometer described below. The HPLC conditions were the same as described above except that a Luna C18(2) column (250 x 2.0 mm, 5 μm) was used and the mobile phase was delivered at 0.3 mL/min. For hydrogen-deuterium exchange experiments, D_2O was substituted for water in mobile phase A and CD_3OD was substituted for methanol in mobile phase B. During LC/MS sample analysis, up to 10 min of the initial flow was diverted away from the mass spectrometer prior to evaluation of metabolites. For some LC/MS analyses, radioactivity was simultaneously monitored with a Radiomatic 150TR radioactivity flow detector (PerkinElmer) to estimate retention times of radiolabeled metabolites in LC/MS data. Flow from the HPLC was split between the mass spectrometer and radioactivity detector such that the flow rate to the mass spectrometer was approximately 100 μL/min.

A Micromass Q-TOF API-US mass spectrometer (Waters Corp.) equipped with an electrospray ionization source and operated in the positive ionization mode was used for metabolite identification. The capillary voltage was 2.0 kV and the cone voltage was 30 V. The collision offset for MS/MS analysis was 20-30 eV. The source block temperature and the desolvation gas temperature were set at 120 and 350 ^{o}C, respectively. The desolvation gas flow and the cone gas

flow were 950 and 50 L/h, respectively. The collision gas pressure setting was 13 psig. TOF MS resolution (m/Δm) was about 8,000, and the RF setting was 0.2. Micromass MassLynx software (version 4.0, Waters Corp.) was used for analysis of LC/MS data. Microsoft Excel 2000 was used for calculations.

NMR Spectroscopy. Synthetic MNTX metabolites were dissolved in CD_3OD (160 μL) and transferred to an NMR tube (3 mm OD). For purpose of comparison, a saturated MNTX solution was also prepared in CD_3OD. Data were collected on Varian Inova 500 MHz and Bruker Avance 600 MHz spectrometers each equipped with a 3mm z-gradient indirect detection probe. One-dimensional (1D) proton (^1H) NMR data and two-dimensional (2D) gCOSY, TOCSY, ^1H-^{13}C gHSQC and ^1H-^{13}C gHMBC NMR data were acquired. All spectra were referenced to the signal of CHD_2OD at 3.32 ppm in the ^1H spectra and 48.1 ppm in the ^{13}C spectra. All spectra were measured at room temperature.

RESULTS

Human study

Six male subjects were enrolled in this study to evaluate the pharmacokinetics of MNTX, total radioactivity in plasma, to determine the urinary and fecal recovery of radioactivity and to characterize the metabolite profiles of MNTX. Each subject was administered a single 0.3 mg/kg (100 μCi) dose of [^{14}C]MNTX as a one-minute intravenous infusion and all 6 subjects completed the study. Renal excretion was the primary route of elimination of total radioactivity, with mean total percent excretion of 53.6. Fecal recovery in the 0-168 hr collection period was 17.3 %. Exhaled $^{14}CO_2$ accounted for less than 0.06% of administered radioactivity in all subjects.

Metabolite Profiles in Plasma

Metabolite profiles of extracts of plasma samples obtained from mice, rats, dogs and humans at 1 h after a single bolus IV dose of radiolabeled MNTX are shown in Figure 2. The recovery of radioactivity into methanol was greater than 80% for all four species. The metabolites in plasma were identified based on the retention times of the synthetic reference standards, where available and LC/MS/MS fragmentation patterns.

Following a single 0.3 mg/kg IV administration of [^{14}C]MNTX to healthy human volunteers, unchanged MNTX was the major drug-related component in pooled plasma, representing 90.3, 79.2, 67.2 and 33.0 % of plasma radioactivity at 0.25, 0.5, 2 and 4 h post-dose, respectively. Plasma metabolites included MNTX-3-sulfate (M2, 0.7-25.0% of total plasma radioactivity), methyl-6α-naltrexol (M4, 0.6-11.9%) and methyl-6β-naltrexol (M5, 0.5-7.0%). Other minor (each less than 6% of plasma radioactivity) radioactive peaks observed in plasma extracts were

not characterized due to low concentrations. Profiles determined in samples collected after 4 h are not reported due to low levels of radioactivity. Naltrexone, the *N*-demethylation product and its metabolite 6β-naltrexol were not detected in plasma of humans, as determined by an LC-MS method. The limit of detection was estimated to be about 6 ng/mL for naltrexone and 3 ng/mL for 6β-naltrexol.

Following a single 5 mg/kg IV dose of [^{14}C]MNTX to mice, the parent compound represented 40.8, 20.2 and 25.7% of total plasma radioactivity at 0.25, 1 and 4 h post-dose, respectively. MNTX metabolites in pooled mouse plasma included methyl-6β-naltrexol (M5), 2-hydroxy-3-*O*-methyl MNTX (M6), MNTX-3-glucuronide (M9) and 2-hydroxy-3-*O*-methyl MNTX glucuronide (M10). These metabolites were characterized by LC/MS as described below. MNTX-3-glucuronide (M9) and 2-hydroxy-3-*O*-methyl MNTX glucuronide (M10) were the most abundant plasma metabolites, representing 30.2-43.5% and 6.6-24.6% of the total radioactivity, respectively, between 0.25 and 4 h post-dose. Following hydrolysis with β-glucuronidase, MNTX-3-glucuronide (M9) and 2-hydroxy-3-*O*-methyl MNTX glucuronide (M10) were almost completely converted to MNTX and 2-hydroxy-3-*O*-methyl MNTX (M6), respectively (Figure 3). Other metabolites observed in plasma were not characterized due to low concentrations.

MNTX was metabolized to a lesser extent in rats compared to mice following a single 5 mg/kg IV administration of [^{14}C]MNTX. The parent drug represented 93.2, 69.3 and 49.8% of total radioactivity at 0.25, 1 and 4 h post-dose, respectively. MNTX-3-sulfate (M2) and MNTX-3-glucuronide (M9) were the most abundant metabolites in pooled plasma, and the percentage of radioactivity attributed to these metabolites increased over time between 0.25 and 4 h,

representing 1.1-18.3% and 2.5-16.9% of total radioactivity, respectively. Small amounts (each ≤ 6% of plasma radioactivity) of methyl-6β-naltrexol (M5) and 2-hydroxy-3-*O*-methyl MNTX (M6) were also observed in plasma. Trace amounts of other metabolites observed in plasma were not characterized due to low concentrations.

Following a single 5 mg/kg IV administration of [^{3}H]MNTX to dogs, MNTX was the major radioactive component in pooled plasma, representing 98.6, 77.2 and 66.4% of total radioactivity at 0.25, 1 and 4 h post-dose, respectively. MNTX-3-glucuronide (M9) was the only major metabolite in plasma, increasing over time, and represented 0-18.5% of total radioactivity in the 0.25 to 4 h period. Several other radioactive peaks (each ≤ 9% of plasma radioactivity) observed in dog plasma were not characterized due to low concentrations.

Metabolite Profiles in Urine

An average of 49.8% of the administered dose was recovered in 0-24 h human urine. The metabolite profile (Figure 4) of the pooled 0-24 h urine was similar to the plasma profiles in humans. MNTX represented about 82% of urinary radioactivity, while MNTX-3-sulfate (M2), methyl-6α-naltrexol (M4) and methyl-6β-naltrexol (M5) represented 4.3, 9.4 and 2.6% of urinary radioactivity, respectively. Radioactivity concentrations were too low to determine accurate metabolic profiles in samples after 24 h.

In mice, a mean of 56.4% of the administered IV dose was excreted in 0-24 h urine. The parent drug represented 83.4% of total radioactivity in the pooled 0-24 h urine sample and the urinary metabolite profile (Figure 4) was qualitatively similar to plasma profiles. Urinary metabolites

included methyl-6β-naltrexol (M5, 2.3% of total radioactivity), 2-hydroxy-3-*O*-methyl MNTX (M6, 3.9%), MNTX-3-glucuronide (M9, 6.5%) and 2-hydroxy-3-*O*-methyl MNTX glucuronide (M10, 2.7%). MNTX-3-glucuronide (M9) and 2-hydroxy-3-*O*-methyl MNTX glucuronide (M10) isolated from mouse urine were also completely hydrolyzed by β-glucuronidase to MNTX and 2-hydroxy-3-*O*-methyl MNTX (M6), respectively (data not shown).

A mean of 56.8% of the administered dose was excreted in 0-24 h rat urine. The parent drug represented 92.4% of total radioactivity in the pooled 0-24 h urine sample and the urinary metabolite profile (Figure 4) was also qualitatively similar to plasma profiles. Urinary metabolites included MNTX-3-sulfate (M2), MNTX-3-glucuronide (M9), methyl-6β-naltrexol (M5) and 2-hydroxy-3-*O*-methyl MNTX (each ≤ 3% of urine radioactivity).

In dogs, about 66.0% of the administered dose was excreted in 0-24 h urine. The metabolite profile (Figure 4) of the pooled 0-24 h urine was similar to the plasma profiles, and MNTX-3-glucuronide (M9) was the only metabolite in urine, representing 3.2% of total radioactivity.

Metabolite Synthesis and Characterization

MNTX. MNTX eluted at about 23 min. Mass spectral data for MNTX was obtained for comparison with its metabolites, and these data are summarized in Table 1. For MNTX, a molecular ion, $[M]^+$, was observed at *m/z* 356. LC/MS with deuterated solvents in the mobile phase generated an $[M]^+$ at *m/z* 358 (data not shown). This finding was consistent with the two exchangeable protons of MNTX present on each of the two hydroxyl groups. The MS/MS spectrum obtained from collision activated dissociation of *m/z* 356 from MNTX with the

proposed fragmentation scheme is shown in Figure 5A. Loss of H_2O from $[M]^+$ generated *m/z* 338 and indicated the presence of an aliphatic hydroxyl group. Loss of the three atoms of the bridging unit (i.e., carbon-carbon-nitrogen) produced a methyl-ethyl-cyclopropylmethylamine ion at *m/z* 112. Cleavage of the cyclopropylmethylene carbon–nitrogen bond with charge retention on the carbon or nitrogen gave *m/z* 55, representing the cyclopropylmethylene group, and *m/z* 302, respectively. Subsequent loss of H_2O from *m/z* 302 yielded *m/z* 284, which further expelled methylvinylamine (CH_2=CHNHCH_3) to give *m/z* 227. Loss of a molecule of CO from *m/z* 227 generated *m/z* 199.

MNTX-3-sulfate (M2). Metabolite M2 eluted at about 14 min. The $[M]^+$ for M2 was observed at *m/z* 436, which was 80 Da larger than MNTX. LC/MS conducted with deuterated solvents in the mobile phase produced $[M]^+$ at *m/z* 438 (data not shown). This finding was consistent with two exchangeable hydrogens for M2, the same as for MNTX. The proposed fragmentation scheme and product ions of *m/z* 436 mass spectrum for M2 are shown in Figure 5B. Neutral loss of 80 Da from $[M]^+$ produced *m/z* 356, the $[M]^+$ for MNTX, indicating that M2 was an MNTX-3-sulfate. Product ions at *m/z* 338, 302, 284, and 55 were also observed for MNTX, which indicated an otherwise unchanged MNTX molecule. The product ion at *m/z* 382 was 80 Da larger than the corresponding ion at *m/z* 302 for MNTX, which was consistent with sulfation of either hydroxyl group of MNTX. Based on observation of neutral loss of H_2O from $[M]^+$ to generate *m/z* 418, consistent with a free aliphatic hydroxyl group, it was proposed that M2 was an aromatic sulfate. Assignment of the protons in the ^{1}H NMR spectrum of synthetic MNTX-3-sulfate are summarized in Table 2. The key protons H-1 and H-2, with chemical shifts far apart in comparison with MNTX, where they are overlapped, and a J coupling of 8.36 Hz suggest sulfation at the 3-hydroxyl group instead of the 14-hydroxyl group (Table 2). The HPLC

retention time and LC/MS spectra of the synthetic MNTX-3-sulfate matched that for M2 observed in human plasma following IV administration. Therefore, M2 was identified as MNTX-3-sulfate.

Methyl-6α-naltrexol (M4) and methyl-6β-naltrexol (M5). Carbonyl reduction metabolites M4 and M5 eluted at approximately 20.5 and 25.5 min, respectively. The $[M]^+$ for both M4 and M5 were observed at *m/z* 358, which was 2 Da larger than the $[M]^+$ for MNTX. LC/MS conducted with deuterated solvents in the mobile phase produced $[M]^+$ at *m/z* 361 (data not shown). This finding was consistent with three exchangeable hydrogens for M4 and M5, one more than for MNTX, and was consistent with the introduction of an additional hydroxyl group. The proposed fragmentation scheme and product ions of *m/z* 358 mass spectrum for M4 are shown in Figure 5C. The fragmentation of M5 (data not shown) was identical to M4. Product ions at *m/z* 112 and 55 were also present for MNTX and indicated unchanged methyl-ethyl amine and cyclopropylmethylene groups. The product ions at *m/z* 304, 286 and 229 were 2 Da larger than the corresponding ions for MNTX and together with the absence of a loss of CO from *m/z* 229 indicated the carbonyl group had been reduced. In a chemical reaction, MNTX completely disappeared after reduction by sodium borohydride, and two products were formed in a ratio of approximately 90:10 (Figure 6). ^{1}H NMR analysis indicated the reduction of the carbonyl group (Table 2). These two synthetic epimers were differentiated by 2D NOESY spectra, which demonstrated key crosspeaks between protons H-5 and H-6 with a coupling constant of 4.9 Hz for the α-epimer (Figure 7), but much weaker crosspeaks between protons H-5 and H-6 with a coupling constant of 6.5 Hz for the β-epimer (data not shown). HPLC retention time and mass spectral data for synthetic methyl-6α-naltrexol and methyl-6β-naltrexol matched that for M4 and

M5, respectively. Therefore, M4 and M5 were identified as the α- and β-epimer of reduced MNTX, respectively.

Metabolite M6. Metabolite M6 eluted at about 24.5 min. The $[M]^+$ for M6 was observed at *m/z* 386, 30 Da larger than the $[M]^+$ for MNTX. LC/MS conducted with deuterated solvents in the mobile phase produced $[M]^+$ at *m/z* 388 (data not shown), indicating two exchangeable hydrogens for M6, identical to MNTX. The proposed fragmentation scheme and product ions of *m/z* 386 mass spectrum for M6 are shown in Figure 8A. Product ions at *m/z* 112 and 55 were also present for MNTX and indicated unchanged methyl-ethyl amine and cyclopropylmethylene groups. Loss of H_2O from $[M]^+$ produced *m/z* 368, which was consistent with an aliphatic hydroxyl group. The product ions at *m/z* 332, 314, 257 and 229 were 30 Da larger than the corresponding ions for MNTX, and together with the absence of loss of methanol from $[M]^+$, indicated that hydroxylation and methylation of a hydroxyl group had occurred on the phenyl moiety. Therefore, M6 was tentatively identified as 2-hydroxy-3-*O*-methyl MNTX.

Metabolite M9. Metabolite M9 eluted at about 12 min. The $[M]^+$ for M9 was observed at *m/z* 532, 176 Da larger than the $[M]^+$ for MNTX indicating M9 was a conjugate. LC/MS conducted with deuterated solvents in the mobile phase produced $[M]^+$ at *m/z* 537 (data not shown), indicating five exchangeable hydrogens for M9, consistent with a glucuronide. The proposed fragmentation scheme and product ions of *m/z* 532 mass spectrum for M9 are shown in Figure 8B. Neutral loss of 176 Da from $[M]^+$ produced *m/z* 356, identical to the $[M]^+$ for MNTX, indicating that M9 was a glucuronide. The product ions at *m/z* 302, 284 and 55 were also observed for MNTX and indicated an otherwise unchanged MNTX molecule. Therefore, M9 was identified as MNTX-3-glucuronide.

Metabolite M10. Metabolite M10 eluted at about 14.1 min. The $[M]^+$ for M10 was observed at *m/z* 562, 190 Da larger than the $[M]^+$ for MNTX and also 176 Da larger than the $[M]^+$ for a 2-hydroxy-3-*O*-methyl MNTX metabolite, M6, described above. LC/MS conducted with deuterated solvents in the mobile phase produced $[M]^+$ at *m/z* 567 (data not shown), indicating five exchangeable hydrogens for M10. The proposed fragmentation scheme and product ions of *m/z* 562 mass spectrum for M10 are shown in Figure 8C. Neutral loss of 176 Da from $[M]^+$ produced *m/z* 386, identical to the $[M]^+$ for M6, indicating that M10 was a glucuronide conjugate. The product ion at *m/z* 55 was also observed for MNTX indicating an unchanged cyclopropylmethylene group. The product ions at *m/z* 332 and 314 were 30 Da larger than the corresponding ions for MNTX, consistent with methylation and hydroxylation as was observed for M6. Enzymatic hydrolysis with β-glucuronidase converted MNTX-3-glucuronide (M9) and M10 to MNTX and 2-hydroxy-3-*O*-methyl MNTX (M6), respectively, indicating the M10 was a glucuronide of M6 (data not shown). Therefore, M10 was tentatively identified as 2-hydroxy-3-*O*-methyl MNTX glucuronide.

DISCUSSION

In this study, comparative metabolism of MNTX was established in humans and the non-clinical safety models used for the development of this drug, which included mice, rats and dogs. The proposed metabolic pathways of MNTX in mice, rats, dogs and humans are shown in Figure 9. The pathways are based on the metabolite profiles observed in plasma and urine. Metabolite profiles of MNTX appeared to be qualitatively similar in plasma and urine for each of the species examined. The primary pathways of metabolism in humans include sulfation at the phenolic group and carbonyl reduction. The mean plasma AUC(0-12) ratio of unchanged MNTX, as measured by a validated bio-analytical method, to total radioactivity was 0.59. This observation along with the urinary and fecal metabolite profiles has suggested the pharmacokinetic differences between the parent compound and metabolites. The overall recovery of the radioactivity in urine and feces accounted for 70.9% of the administered radioactive dose. Urinary recovery in the 0-24 he period was 43.9%. In this collection interval, MNTX accounted for 37.1% of the administerd dose; M2, M4 and M5 represented 1.26, 4.25 and 0.74%, respectively. About 17.3 % of the dose was recovered in the feces (0-168 hrs). In this collection interval, MNTX accounted for 11.4% of administered dose in the feces; M4 and M5 represented 0.83 and 0.24% of the dose, respectively. M2 was not observed in feces.

N-Demethylation leading to the formation of naltrexone and its reduction product 6β-naltrexol did not appear to be a significant pathway of metabolism for MNTX in humans, since these metabolites were not observed in plasma or urine. Trace amounts of radioactivity excreted in exhaled CO_2 (<0.06% of a total dose) provided a strong indication that N-demethylation represents a negligible metabolic pathway of MNTX in humans. These results confirmed an earlier observation that *N*-demethylation was not a major metabolic pathway of MNTX in cancer

patients (Kotake et al., 1989). Thus, potential impairment of analgesic effects of opioids through *N*-demethylation of MNTX in humans can be ruled out. In male rats, the metabolic pathways of MNTX were sulfation, glucuronidation, hydroxylation and methylation. MNTX was more extensively metabolized in mice than in rats, dogs and humans via glucuronidation, reduction, hydroxylation and methylation. MNTX was metabolized in dogs primarily via glucuronidation of the phenol.

There appeared to be some major differences between MNTX and naltrexone in terms of metabolism in humans and laboratory animals. In humans, in addition to the presence of 6β-naltrexol in conjugated and non-conjugated forms and conjugated naltrexone as the major metabolites, 2-hydroxy-3-*O*-methylnaltrexone, 3-*O*-methyl-6β-naltrexol and 2-hydroxy-3-*O*-methyl-6β-naltrexol were reported as minor or trace metabolites of naltrexone (Cone et al., 1978; Wall et al., 1981). These metabolites were also detected in animal species along with 6α-naltrexol, 3-*O*-methylnaltrexone and some dealkylation products (Misra et al., 1976; Rodgers et al., 1980; Misra, 1981), which were not observed in humans. A study in dogs showed that naltrexone was predominantly excreted as the 3-glucuronide. MNTX was metabolized via glucuronidation, hydroxylation, methylation, sulfation and carbonyl reduction in non-clinical species. Although both drugs appeared to be primarily metabolized via conjugation of the phenolic group and reduction of the ketone in humans, both 6α- and 6β- epimers of the reduced MNTX isomers, were observed for MNTX only in human plasma . Also, the extent of metabolism was much higher for naltrexone than for MNTX in humans. For example, following a subcutaneous administration of naltrexone, 6β-naltrexol represented about 40% of the administrated dose while the parent drug represented only about 10% of the administrated dose

(Wall et al., 1984), based on AUC values. In contrast to naltrexone, the carbonyl reduction metabolites M4 and M5 of MNTX represented less than 10% of total plasma radioactivity, based on AUC values following a single IV administration of MNTX at 0.3 mg/kg.

In summary, MNTX was not extensively metabolized in humans following a single IV administration. Conversion to methyl-6-naltrexol isomers (M4 and M5) and MNTX-3-sulfate (M2) were the primary pathways of metabolism. MNTX was more extensively metabolized in mice compared to rats, dogs, and humans through glucuronidation, reduction, hydroxylation and methylation. MNTX-3-glucuronide (M9) was a major metabolite in plasma of mice, rats and dogs, but was not observed in human plasma. 2-Hydroxy-3-*O*-methyl MNTX glucuronide (M10) was a major metabolite in mouse plasma, but was absent in circulation of other species. MNTX-3-sulfate (M2) was the major metabolite in rat and human plasma. However, this metabolite was not observed in other species. 2-Hydroxy-3-*O*-methyl MNTX (M6) was observed in the circulation of mice and rats, but was not detected in the circulation of dogs and humans. Methyl-6α-naltrexol (M4) and methyl-6β-naltrexol (M5), the reduced MNTX isomers, were both observed in human plasma. However, only methyl-6β-naltrexol (M5) was observed in the plasma of mice and rats, and neither isomer was present in dog plasma. *N*-Demethylation resulting in naltrexone formation was not observed in humans. These data suggested species differences in the metabolism of MNTX.

Acknowledgments

The authors would like to thank Daniel Evcic and Andre Negahban for their technical assistance in these studies.

Disclosure: PGNX has a proprietary commercial interest in MNTX. YR is an employee and stockholder of PGNX.

References

Benedetti S, Fraier D, Pianezzola E, Castelli M, Dostert P and Gianni L (1993) Stereoselectivity of iododoxorubicin reduction in various animal species and humans. *Xenobiotica* **23:**115-121.

Benedetti S, Pianezzola E, Fraier D, Castelli M and Dostert P (1991) Stereoselectivity of idarubicin reduction in various animal species and humans. *Xenobiotica* **21:**473-480.

Brown D and Goldberg L (1985) The use of quaternary narcotic antagonists in opiate research. *Neuropharmacology* **24:**181-191.

Cameron J (1992) Constipation related to narcotic therapy: a protocol for nurses and patients. *Cancer Nurs* **15:**372-377.

Chen TY, Rosow CE (2007) Methylnaltrexone bromide. Drugs of the Future 32: 771-775.

Cone E, Gorodetzky C, Darwin W, Carroll F, Brine G and Welch C (1978) The identification and measurement of two new metabolites of naltrexone in human urine. *Research Communication in Chemical Pathology & Pharmacology* **20:**413-433.

Culpepper-Morgan J, Inturrisi C, Portenoy R, Foley K, Houde R, Marsh F and Kreek M (1992) Treatment of opioid-induced constipation with oral naloxone. *Clin. Pharmacol. Ther.* **52:**90-95.

Dayton H and Inturrisi C (1976) The urinary excretion profiles of naltrexone in man, monkey, rabbit, and rat. *Drug Metab Dispos* **4:**474-478.

Dow J and Berg C (1995) Stereoselectivity of the carbonyl reduction of dolasetron in rats, dogs, and humans. *Chirality* **7:**342-348.

Glare P and Lickiss J (1992) Unrecognized constipation in patients with advanced cancer: a recipe for therapeutic disaster. *J Pain Symptom Manage* **7:**369-371.

Hermans J and Thijssen H (1989) The in vitro ketone reduction of warfarin and analogues. Substrate stereoselectivity, product stereoselectivity and species differences. *Biochem Pharmacol* **38:**3365-3370.

Jones D, Jukes-Jones R, Verschoyle R, Farmer P and Gescher A (2005) A synthetic approach to the generation of quercetin sulfates and the detection of quercetin 3'-*O*-sulfate as a urinary metabolite in the rat. *Bioorganic & Medicinal Chemistry* **13:**6727-6731.

Kotake AN, Kuwahara SK, Burton E, McCoy CE, Goldberg LI. (1989) Variations in demethylation of *N*-methylnaltrexone in mice, rats, dogs, and humans. Xenobiotica **19**: 1247-1254.

Kim C, Cheng R, Corrigall WA and Coen KM. (1989) Assay for methylnaltrexone in rat brain regions and serum by high-performance liquid chromatography with coulometric electrochemical detection. Chromatographia **28**: 359-363.

Malspeis L, Bathala M, Ludden T, Bhat H, Frank S, Sokoloski T, Morrison B and Reuning R (1975) Metabolic reduction of naltrexone I. Synthesis, separation and characterization of naloxone and naltrexone reduction products and qualitative assay of urine and bile following administration of naltrexone, alpha-naltrexol, or beta-naltrexol. *Research Communication in Chemical Pathology & Pharmacology* **12:**43-65.

Malspeis L, Ludden T, Bathala M, Morrison B, Feller D and Reuning R (1976) Metabolic reduction of naltrexone II. In vitro studies using liver from guinea pig, monkey and rat. *Research Communication in Chemical Pathology & Pharmacology* **14:**393-406.

Misra A (1981) Current status of preclinical research on disposition, pharmacokinetics, and metabolism of naltrexone. *national Institute on Drug Abuse Research Monograph* **28:**132-146.

Misra AL, Pontani RB, Vadlamani NL. (1987) Intravenous kinetics and metabolism of [15,16-3H]naltrexonium methiodide in the rat. J. Pharm. Pharmacol. **39**: 225-227.

Misra A, Bloch R, Vardy J, Mule S and Verebely K (1976) Disposition of [15,16-^{3}H]naltrexone in the central nervous system of the rat. *Drug Metab Dispos* **4:**276-280.

Murphy DB, El Behiery H, Chan VW and Foss Jf. (2001) Pharmacikinetic profile of epidurally administered methylnaltrexone, a novel peripheral opioid anatagonist in a rabbit model. British J. Anaesthesis **86**: 120-2.

Porter S, Somogyi A and White J (2000) Kinetics and inhibition of the formation of 6β-naltrexol from naltrexone in human liver cytosol. *Br J Clin Pharmacol* **50:**465-471.

Rodgers R, Taylor S, Dickinson R, Ilias A, Lynn R and Gerber N (1980) Metabolism and choleretic effect of naltrexone in the isolated perfused rat liver. *Drug Metab Dispos* **8:**390-396.

Sykes N (1991) Oral naloxone in opioid-associated constipation. *Lancet* **337:**1475

Thomas J, Karver S, Cooney GA, Chamberlain BH, Watt CK, Slatkin NE, Stambler N, Kremer AB and Israel RJ (2008). Methylnaltrexone for opioid-induced constipation in advanced illness. New Eng. J. Med. **358**: 2332-43.

Vickers S, Duncan C, Kari P, Homnick C, Elliott J, Pitzenberger S, Hichens M and Vyas K (1993) In vivo and in vitro metabolism studies on a class III antiarrhythmic agent. *Drug Metab Dispos* **21:**467-473.

Wall M, Brine D and Perez-Reyes M (1981) Metabolism and disposition of naltrexone in man after oral and intravenous administration. *Drug Metab Dispos* **9:**369-375.

Wall M, Perez-Reyes M, Brine D and Cook C (1984) Naltrexone disposition in man after subcutaneous administration. *Drug Metab Dispos* **12:**677-682.

Weil A, Caldwell J, Guichard J and Picot G (1989) Species differences in the chirality of the carbonyl reduction of [14C]fenofibrate in laboratory animals and humans. *Chirality* **1:**197-201.

Yuan C, Foss J, Moss J and Roizen M (1998) Gut motility and transit changes in patients receiving long-term methadone maintenance. *J Clin Pharmacol* **38:**931-935.

Yuan C, Foss J, O'Connor M, Toledano A, Roizen M and Moss J (1996) Methylnaltrexone prevents morphine-induced delay in oral-cecal transit time without affecting analgesia: a double-blind randomized placebo-controlled trial. *Clin. Pharmacol. Ther.* **59:**469-475.

Yuan C, Wei G, Foss J, O'Connor M, Karrison T and Osinski J (2002) Effects of subcutaneous methylnaltrexone on morphine-induced peripherally mediated side effects: a double-blind randomized placebo-controlled trial. *J Pharmacol. Exp. Ther.* **300:**118-123.

Footnotes

Address correspondence to: Dr. Appavu Chandrasekaran, Pharmacokinetics, Dynamics and Metabolism, Pfizer Inc., 500 Arcola Road, Collegeville, PA 19426. E-mail: Chandra@wyeth.com

Legends for Figures

Figure 1. Structure of methylnaltrexone bromide. * indicates the site of the ^{14}C label. **T** indicates the site of the ^{3}H labels

Figure 2. Metabolite profiles of MNTX in plasma of mice, rats, dogs and humans 1 hour after a single bolus IV administration

Figure 3. Hydrolysis of 1 h mouse plasma sample by ß-glucuronidase

Figure 4. Metabolite profiles of MNTX in pooled 0-24 hr urine of mice, rats, dogs and humans

Figure 5. Product ion mass spectra of MNTX, M2 and M4

Figure 6. Formation of methyl-6-naltrexol epimers by reduction of MNTX with sodium borohydride

Figure 7. 2D NOESY NMR spectra of methyl-6α-naltrexol (M4) with key crosspeaks between protons H-5 and H-6 (circled)

Figure 8. Product ion mass spectra of M6, M9 and M10

Figure 9. Metabolic pathways of MNTX in mice, rats, dogs and humans

Table 1. Retention times and mass spectral properties for MNTX and its metabolites observed in mice, rats, dogs and humans

Metabolite	t_R (min)	Molecular ion (M^+) (*m/z*) with H_2O	with D_2O	Relevant Product Ions (*m/z*)
MNTX	23.0	356	358	338, 302, 284, 227, 199, 112, 55
M2	14.0	436	438	418, 382, 356, 302, 284, 227, 199, 112, 55
M4	20.5	358	361	340, 304, 286, 229, 201, 112, 55
M5	25.5	358	361	340, 304, 286, 229, 201, 112, 55
M6	24.5	386	388	368, 332, 314, 257, 229, 112, 55
M9	12.0	532	537	356, 302, 284, 227, 199, 113, 55
M10	14.1	562	567	386, 332, 314, 257, 229, 113, 55

Table 2. Chemical shifts of MNTX and its synthetic MNTX metabolite standards

Proton #	MNTX		M2		M4		M5	
	^{1}H	^{13}C	^{1}H	^{13}C	^{1}H	^{13}C	^{1}H	^{13}C
1	6.76	120.23	6.76	119.31	6.69	119.68	6.75	119.5
2	6.77	118.92	7.31	123.62	6.78	118.92	6.77	118.2
3		140.8				139.77		
4		143.6				146.65		
5	4.871	89.09	4.80	88.72	4.72	89.32	4.46	95.11
6		207.72			4.30	65.52	3.57	62.80
7	1.79/2.97	24.57	1.69/2.81	24.2	1.26/1.85	23.07	1.69/2.75	24.73
8	1.79/2.11	32.45	1.62/1.95	32.1	1.71/1.71	30.30	1.57/1.79	31.2
9	4.023	72.44	3.89	71.39	3.94	72.06	3.91	73.40
10	3.64/3.67	27.53	3.09/3.55	27.4	3.21/3.63	28.71	3.16/3.61	28.05
11		119.40				121.48		119.4
12		127.60				130.00		130.0
13		48.9				65.88		45.8
14		72.20				73.08		71.5
15	2.22/3.05	34.25	2.07/2.80	33.87	1.74/2.79	27.10	1.69/2.75	24.53
16	3.04/3.41	57.47	2.85/3.24	57.02	3.15/3.32	57.20	2.97/3.32	57.6
18	2.92/3.96	72.39	2.74/3.88	72.01	2.86/3.99	73.23	2.81/3.96	72.56
19	1.23	3.50	1.14	3.05	1.25	3.93	1.23/1.28	3.59
20	0.49/0.87	2.165	0.311	0.69	0.49/0.85	2.70	0.45/0.83	2.40
21	0.687/0.96	5.51	0.531	0.80	0.66/0.94	5.68	0.66/0.94	6.24
22	3.79	52.91	3.62	52.67	3.70	52.84	3.72	53.58

1

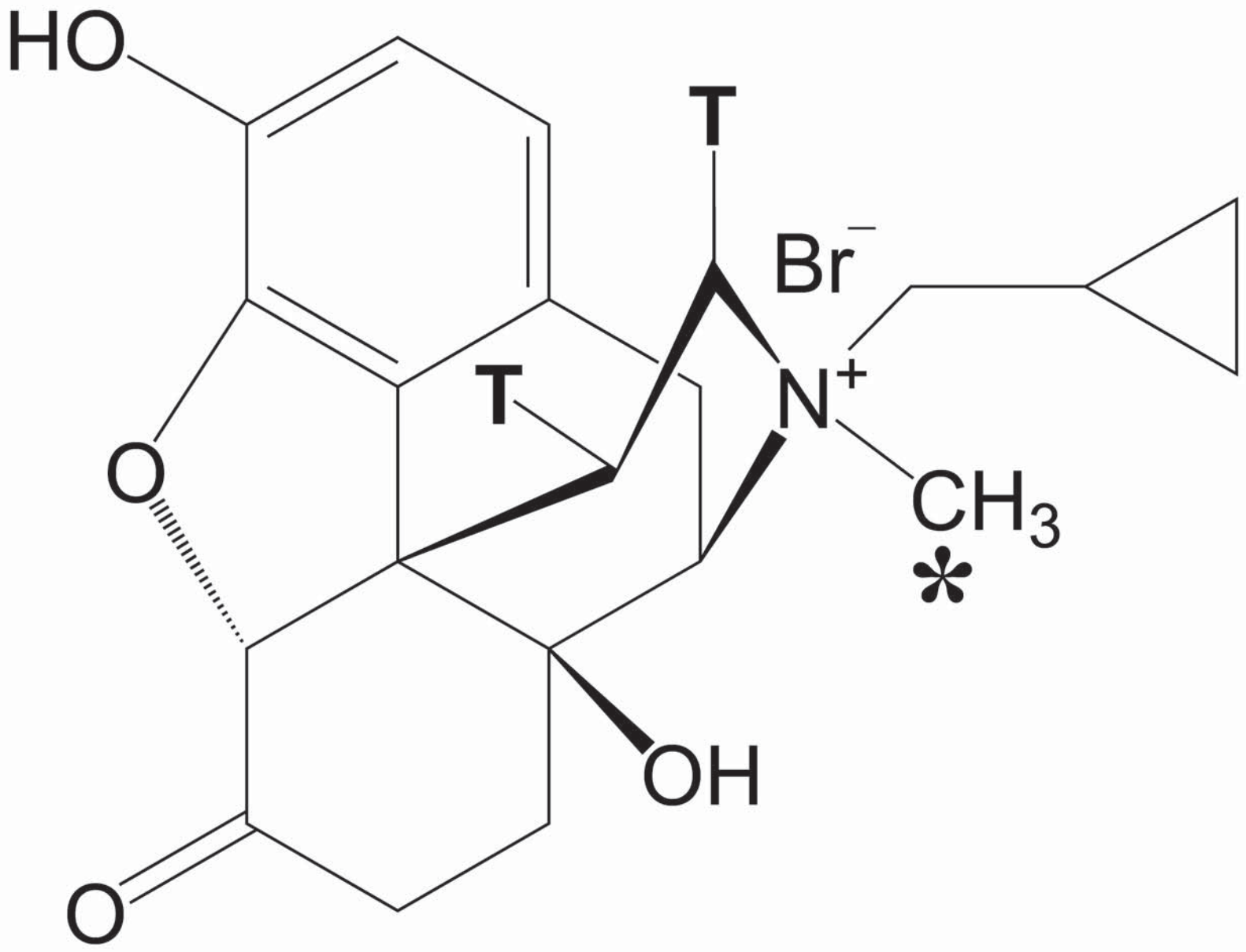

2

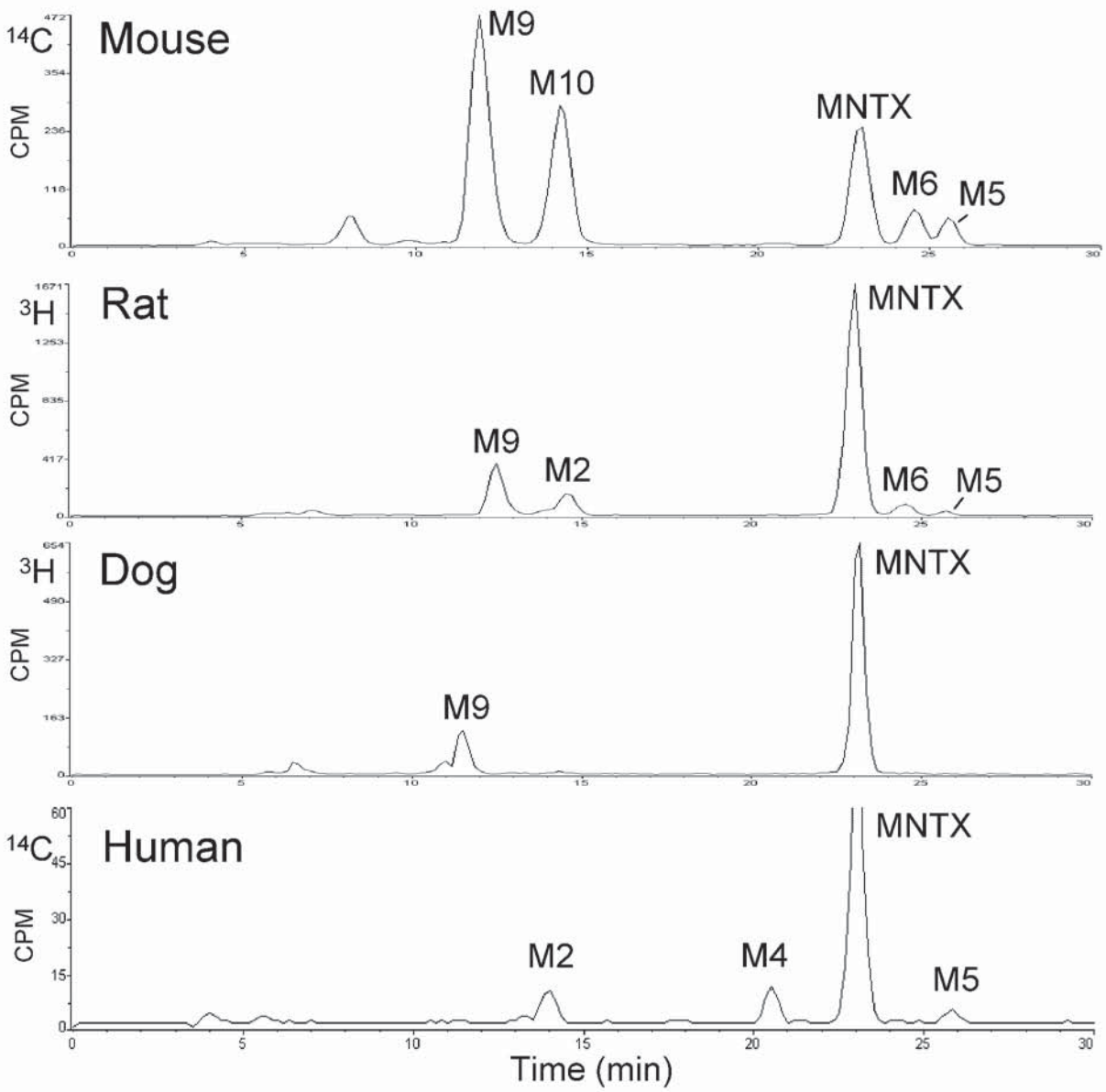
Mouse
M9
M10
MNTX
M6
M5
Rat
MNTX
M9
M2
M6
M5
Dog
MNTX
M9
Human
MNTX
M2
M4
M5
CPM
Time (min)

3

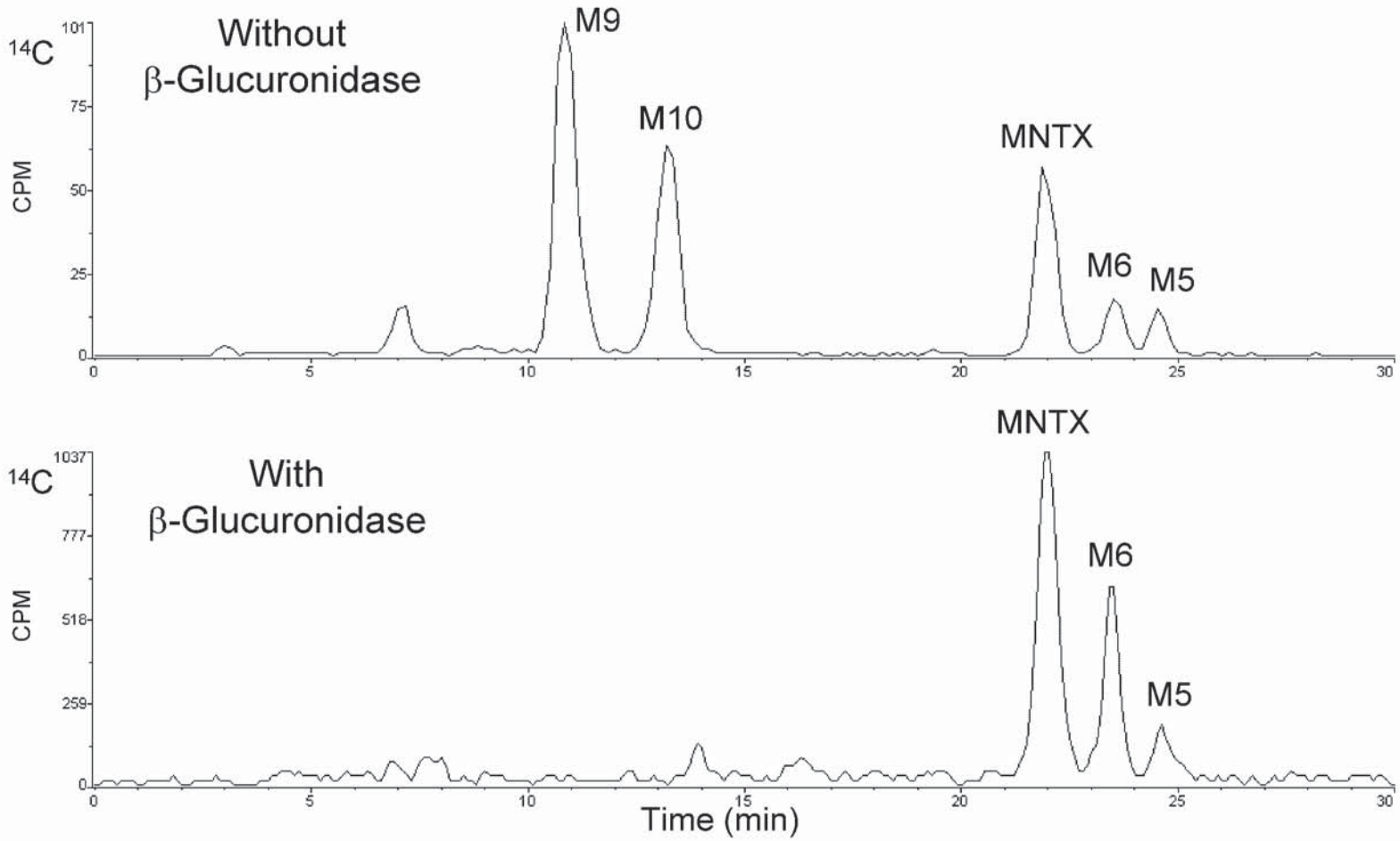
Without
β-Glucuronidase
^{14}C
CPM
101
75
50
25
0
M9
M10
MNTX
M6
M5
0
5
10
15
20
25
30
With
β-Glucuronidase
^{14}C
CPM
1037
777
518
259
0
MNTX
M6
M5
Time (min)

4

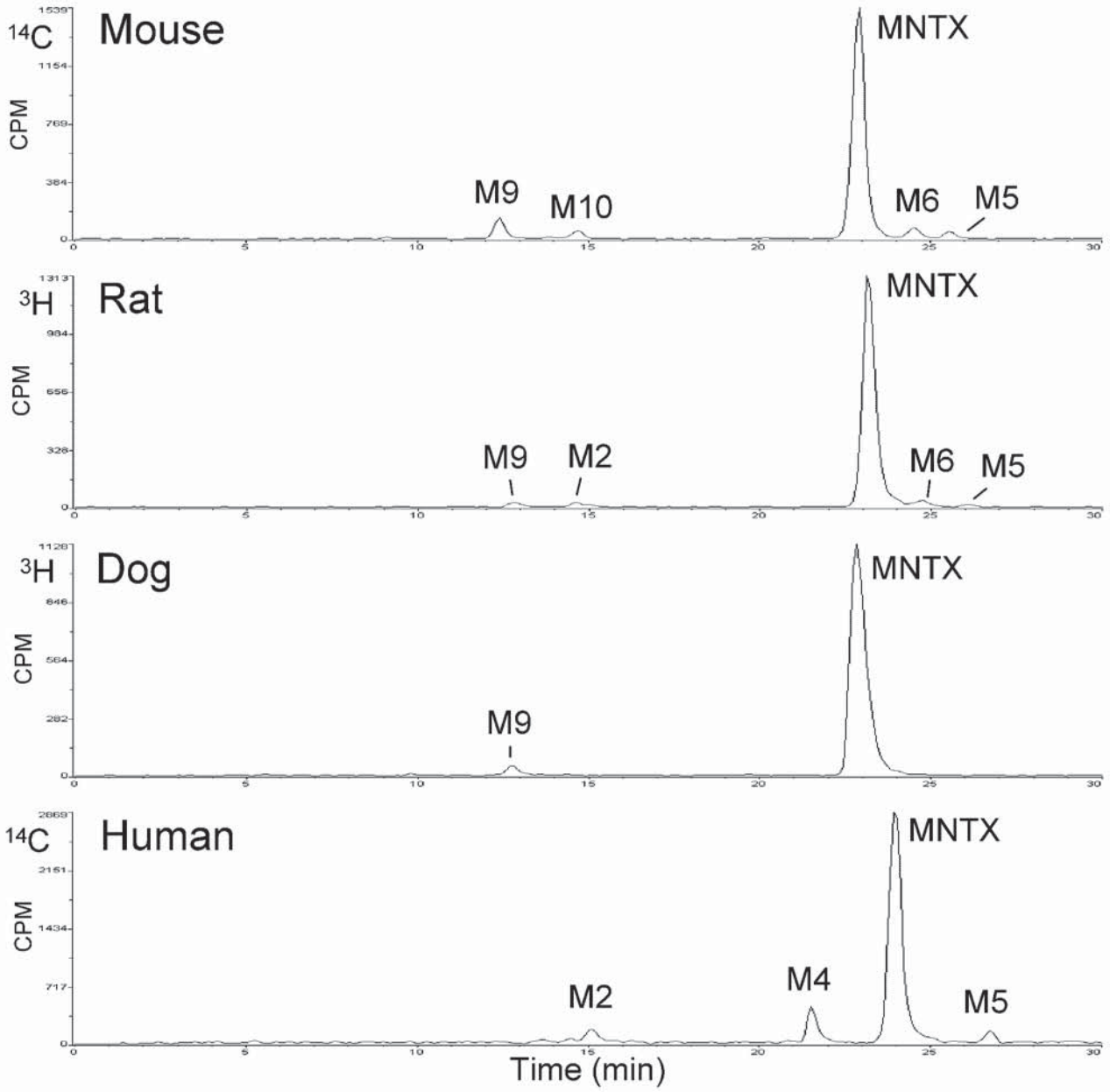
Mouse
^{14}C
CPM
MNTX
M9
M10
M6
M5
Rat
^{3}H
CPM
MNTX
M9
M2
M6
M5
Dog
^{3}H
CPM
MNTX
M9
Human
^{14}C
CPM
MNTX
M2
M4
M5
Time (min)

5

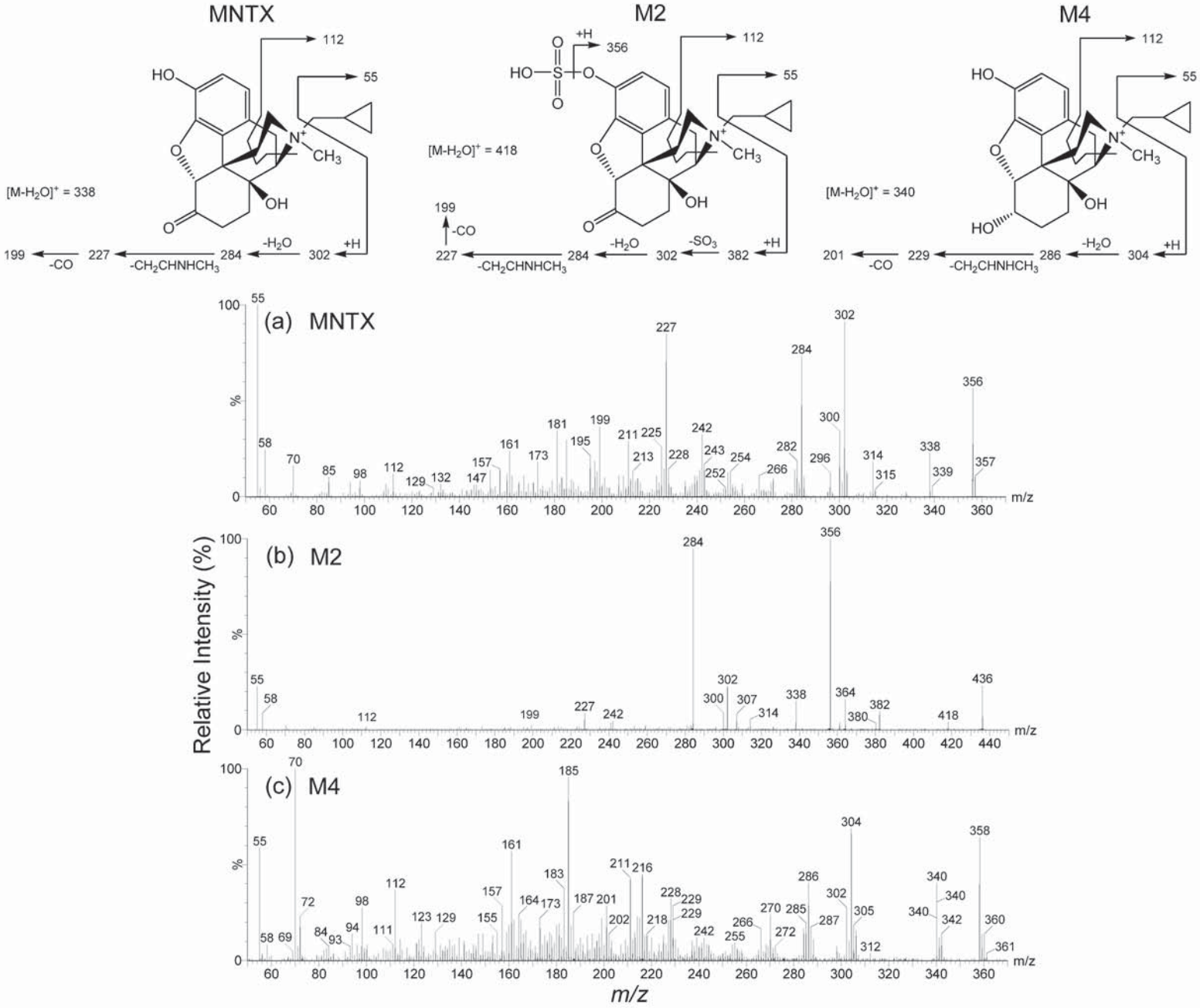
MNTX
M2
M4
[M-H2O]+ = 338
[M-H2O]+ = 418
[M-H2O]+ = 340
-CO
-CH2CHNHCH3
-H2O
-SO3
+H
(a) MNTX
(b) M2
(c) M4
Relative Intensity (%)
m/z

6

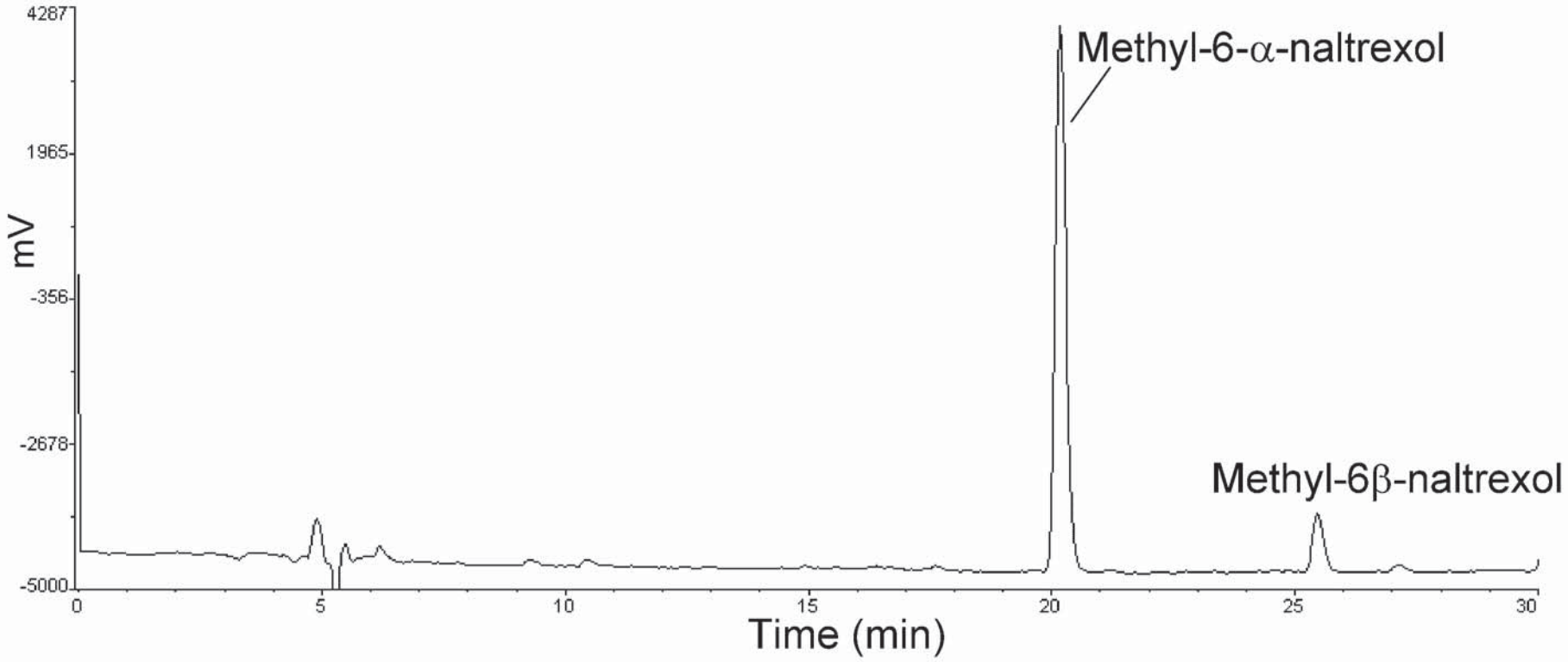
4287
1965
-356
-2678
-5000
mV
0
5
10
15
20
25
30
Time (min)
Methyl-6-α-naltrexol
Methyl-6β-naltrexol

7

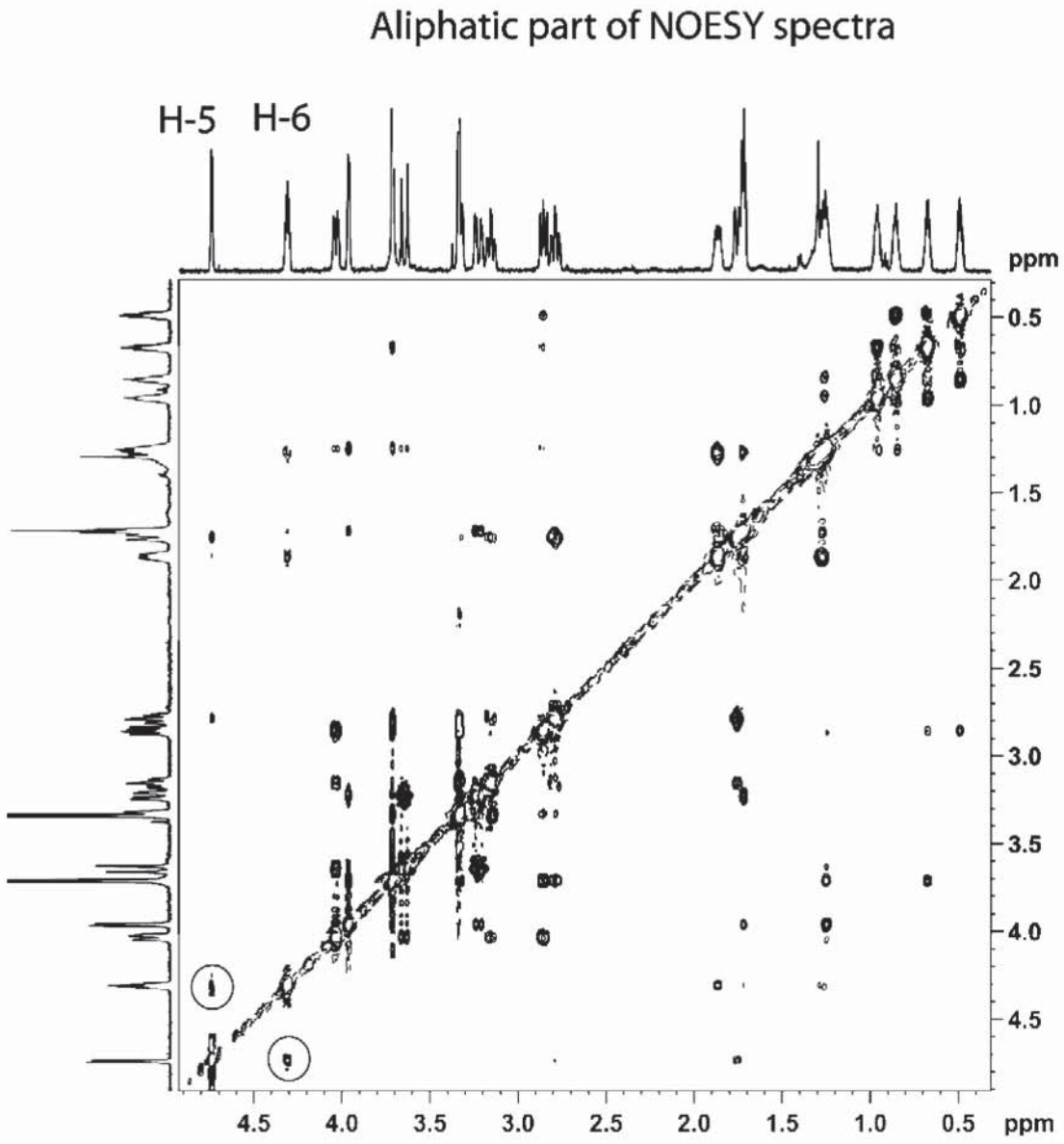
Aliphatic part of NOESY spectra
H-5
H-6
ppm
0.5
1.0
1.5
2.0
2.5
3.0
3.5
4.0
4.5
4.5
4.0
3.5
3.0
2.5
2.0
1.5
1.0
0.5
ppm

8

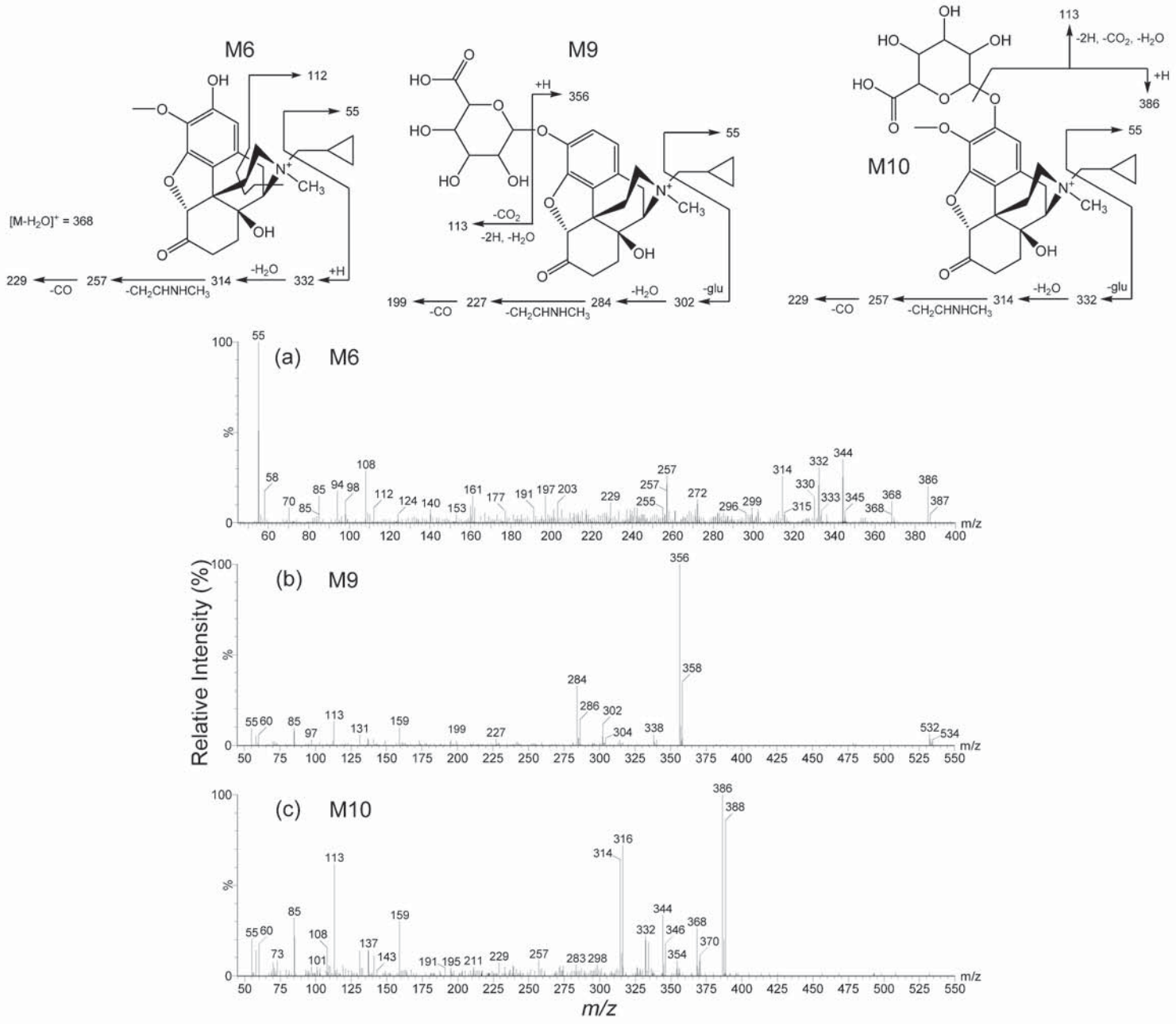
M6
M9
M10
[M-H2O]+ = 368
-CO
-CH2CHNHCH3
-H2O
+H
-glu
-CO2
-2H, -H2O
-2H, -CO2, -H2O
(a) M6
(b) M9
(c) M10
Relative Intensity (%)
m/z

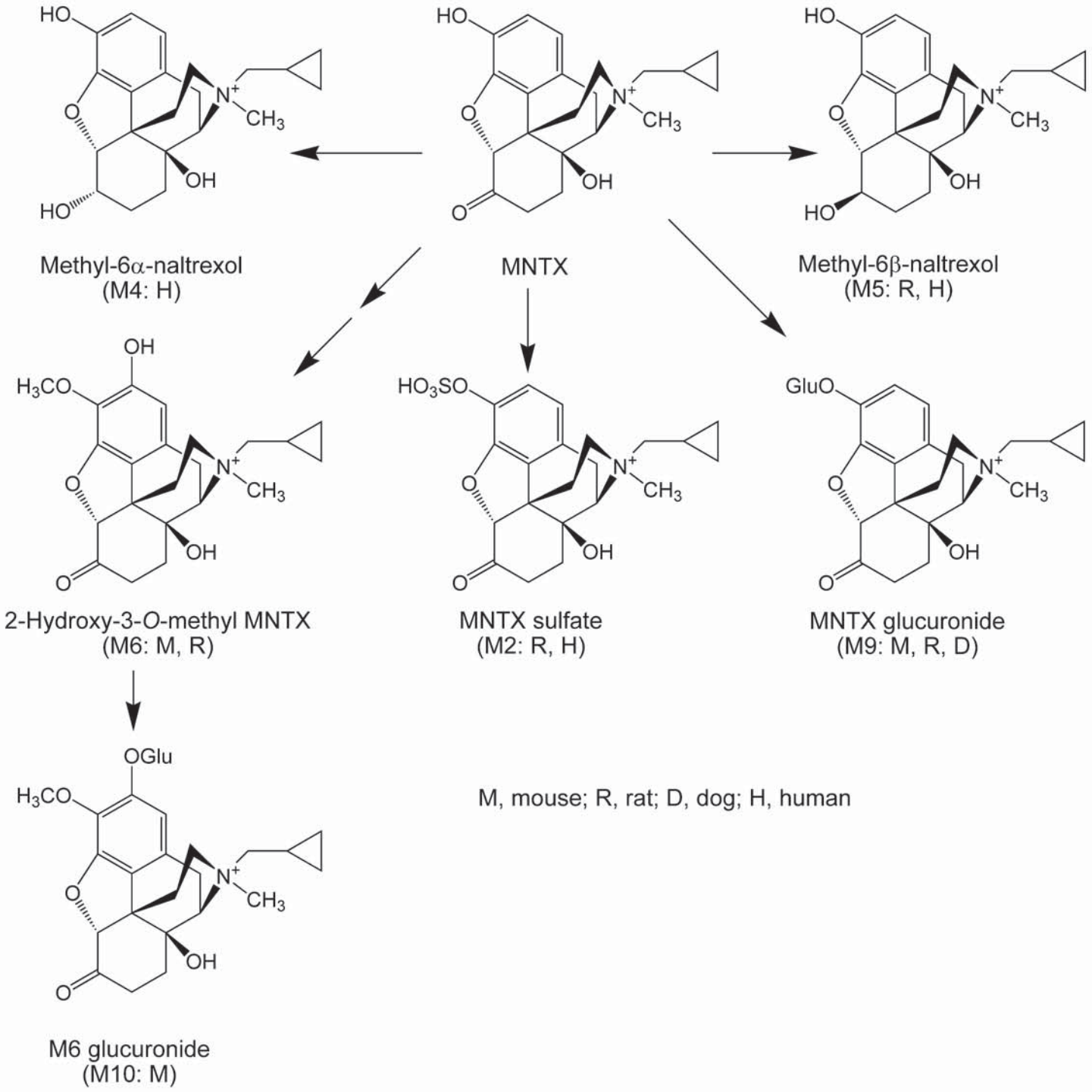
Methyl-6α-naltrexol
(M4: H)
MNTX
Methyl-6β-naltrexol
(M5: R, H)
2-Hydroxy-3-O-methyl MNTX
(M6: M, R)
MNTX sulfate
(M2: R, H)
MNTX glucuronide
(M9: M, R, D)
M6 glucuronide
(M10: M)
M, mouse; R, rat; D, dog; H, human